ôMultiple Fire Index Examination of Future Climate Change Affecting Wildfire Seasonality and Extremes in the Contiguous United States ∅

LEE KESSENICH[®], ^a MELISSA BUKOVSKY, ^b RACHEL MCCRARY, ^a SETH MCGINNIS, ^a LINDA O. MEARNS, ^a JOHN T. ABATZOGLOU, ^c AND ALISON CULLEN^d

a Research Applications Lab, National Center for Atmospheric Research, Boulder, Colorado
b Haub School of Environment and Natural Resources, University of Wyoming, Laramie, Wyoming
c Management of Complex Systems, University of California Merced, Merced, California
d Daniel J. Evans School of Public Policy and Governance, University of Washington, Seattle, Washington

(Manuscript received 9 December 2024, in final form 11 July 2025, accepted 16 October 2025)

ABSTRACT: Climate change is impacting wildfires in the contiguous United States; thus, projections of fire danger under climate change have the potential to inform responses to changing wildfire risks. We calculate fire indices for 13 dynamically downscaled regional climate models, then count days exceeding relevant fire danger thresholds, and compare future changes for mid- and late-twenty-first century relative to a historical reference period. We then compare the responses of the fire indices to highlight areas of agreement and disagreement on the sign and magnitude of future change in fire danger days. Many regions in the domain experience increases in the number of days exceeding fire danger thresholds by the midcentury. The regions which exhibit agreement across the simulation ensemble on the sign of change, and the magnitude of that change, vary greatly between indices. The timing and frequency of fire danger days (defined as days exceeding fire danger thresholds) throughout the year change, both in the shoulder season and during existing peaks in fire danger. By the end of the century, most of the domain experiences statistically significant increases in the number of fire danger days. Complex interactions between input variables, and the sensitivities to inputs, affect the response of fire indices under climate change. The projected increase in fire weather risk could place greater demands upon fire management resources, pose elevated hazards for populations exposed to fire, and potentially disrupt landscapes and infrastructure more frequently.

SIGNIFICANCE STATEMENT: The purpose of this study is to examine future changes in multiple fire indices, calculated for an ensemble of regional climate models, under a high emission scenario for the contiguous United States. We compare the fire indices to one another and examine their responses to climate change to better understand how climate change may impact weather conducive to wildfires. We find that the fire indices do not respond to climate change uniformly and that in the midcentury, some regions disagree on the sign of change, while other regions agree on the sign of change and project increases in fire conducive weather. More frequent fire conducive weather poses challenges for fire management and human safety.

KEYWORDS: Climate change; Uncertainty; Climate models; Climate services; Forest fires

1. Introduction

Future projections of fire potential are needed to anticipate future impacts and inform long-term management practices. Wildfires can be destructive and expensive to manage, particularly near populated areas, where fire suppression is motivated by the protection of life and property. In addition, wildfires can disrupt infrastructure such as roads, utilities, and water supply, and smoke from wildfires negatively affects human health (Black et al. 2017). Existing research establishes the key role of climate and weather in the intensity and spread of wildfires and

Denotes content that is immediately available upon publication as open access.

© Supplemental information related to this paper is available at the Journals Online website: https://doi.org/10.1175/JAMC-D-24-0230.s1.

Corresponding author: Lee Kessenich, kessenic@ucar.edu

confirms that climate change is contributing to changes in wild-fire across the United States (e.g., Goss et al. 2020; Williams et al. 2019; Abatzoglou and Williams 2016; Westerling 2016). Climate change is likely to alter the intensity, season length, and seasonality of fire, which will affect fire management practices, increase competition for regional fire suppression resources, and increase the cost and complexity of risk management and the protection of infrastructure and human health (Jolly et al. 2015; Cullen et al. 2021; Podschwit and Cullen 2020; Cullen et al. 2024).

Wildfires require an ignition source, fuels, and conducive weather conditions to start and spread. Ignitions can be difficult to quantify or predict, but fuel conditions (e.g., dryness) and fire-conducive weather are informed by meteorological conditions. These fuel and fire weather characteristics are often quantified by fire indices that synthesize meteorological variables into a quantification of fire danger potential or fire behavior potential. Indices of fuel moisture and fire characteristics that incorporate temperature, precipitation, and other atmospheric variables can serve as better indicators of macroscale annual area burned than temperature or precipitation alone (Abatzoglou and Kolden 2013). Fire indices have been applied to understand

DOI: 10.1175/JAMC-D-24-0230.1

macroscale changes in fire potential and potential fire behavior (e.g., Baijnath-Rodino et al. 2023; Richardson et al. 2022; Bedia et al. 2015) and are routinely applied to decision-making in fire management (Bradshaw et al. 1983).

Multiple fire indices have been developed to inform fire management systems in different regions of North America and focus on different aspects of fire danger. Fire indices are intended to assist fire management in allocating resources, which is driven by the intensity, timing, and duration of wildland fire. The Canadian Forest Fire Danger Rating System was released in 1970 with fuel moisture and fire behavior indicators for fuel and fire conditions within Canada (Van Wagner 1987). The U.S. National Fire Danger Rating System (NFDRS) was developed to be a scientific- and engineering-based system that would be applicable across the contiguous United States and adaptable to the needs of local management. Its components include measures of fuel moisture, fire intensity, and fire spread (Schlobohm and Brain 2002). Developed separately, but incorporated into and used alongside NFDRS, are the Keetch-Byram drought index (Keetch and Byram 1968) and modified Fosberg fire weather index (Goodrick 2002). These two indices were developed in the southeast United States, which has a different fire regime than the western United States. In 2019, the severe fire danger index was released, intended for decision support for practitioners using NFDRS indices. It correlates to fire activity and firefighter fatalities (Jolly et al. 2019). These indices have inherently different time scales and vary in sensitivity to meteorological inputs, reflecting heterogeneity in their development and intended uses.

Given the diversity of fire indices used operationally and in previous studies (Littell et al. 2016), we calculated projections of a suite of fire indices for a set of dynamically downscaled future climate projections, or regional climate model (RCM) simulations, that cover the contiguous United States (CONUS). The RCM ensemble comes from the North American component of the Coordinated Regional Climate Downscaling Experiment (NA-CORDEX) archive focused on representative concentration pathway 8.5 (RCP8.5) (Mearns et al. 2017; Bukovsky and Mearns 2020). RCP8.5 is characterized by high levels of greenhouse gas emissions and explores a plausible high risk scenario (Terando et al. 2020). While many other RCM-based products are available and widely used, as well as statistically downscaled datasets (e.g., Abatzoglou and Brown 2012), we focus on NA-CORDEX due to its physically based approach and its comparatively robust sampling of structural uncertainties across models. This feature of NA-CORDEX allows us to explore the uncertainty in future changes in fire indices and highlight regions of model agreement. By examining fire indices calculated from an RCM ensemble, we can examine fire-management-relevant metrics of fire season length, timing, and extremes under a high emission climate change scenario. Seasonality is distinct from season length, as seasonality refers to the expected timing of fire throughout the year, whereas season length does not indicate timing. Although ignitions are a vital component of wildfires, modeling wildfire ignitions is outside the scope of this analysis.

Previous research that examined future changes in fire weather primarily focused on examining fire indices individually (e.g., Goss et al. 2020; Flannigan et al. 2013; Wotton and Flannigan 1993; Jain et al. 2017; Tang et al. 2015; Lu et al. 2011; Fox-Hughes et al. 2014), while a few studies included several indices (e.g., Abatzoglou and Williams 2016; Jolly et al. 2015; Yu et al. 2023; Preisler et al. 2008). However, individual indices are not equally applicable across regions; they exhibit different sensitivities to climate change (Flannigan et al. 2016); they were developed to capture different attributes of fire.

In this paper, we calculate projections of future fire weather, as described by a variety of fire indices, for a 13-member ensemble of regional simulations from NA-CORDEX. This work provides an in-depth analysis of fire weather danger across a large and variable domain that includes different fire regimes. Comparing projections of various fire weather indices is an underexplored topic. This analysis expands our understanding of future fire danger under climate change, which is critical for long-term fire management.

2. Datasets, models, and methods

a. gridMET

The gridMET dataset is a gridded surface meteorological dataset that has been validated against multiple networks of weather station data to ensure accuracy to observations. The dataset has a resolution of $1/24^{\circ}$, so to better match our simulation data, we regrid gridMET to a $1/4^{\circ}$ grid using local area averaging. The gridMET dataset provides maximum and minimum temperature, precipitation accumulation, downward surface shortwave radiation, wind velocity, maximum and minimum relative humidity, and specific humidity on a daily time step (Abatzoglou 2013).

b. Regional climate models

Our climate model data are from 13 regional climate model simulations from NA-CORDEX (Mearns et al. 2017; Bukovsky and Mearns 2020). Ten simulations have a grid spacing of 25 km, and three simulations have a grid spacing of 50 km, which have been regridded using local area averaging to a 1/4° or 1/2° common grid, respectively. For ensemble comparison, the 1/2° simulations were regridded to match the $1/4^{\circ}$ simulations using bilinear interpolation. Global climate model (GCM) simulations have finite spatial resolution, especially in areas of complex topography. To better capture spatial and temporal meteorological features important to wildfire, we used RCM simulations that downscale GCMs to higher resolution. These simulations were produced by 6 RCMs downscaling 6 GCMs from the Coupled Model Intercomparison Project phase 5 (CMIP5) in various combinations listed in Table 1. The RCM simulations run from 1950 to 2099, using the RCP8.5 (Moss et al. 2008) for future periods. RCP8.5 is characterized by high levels of greenhouse gas emissions and is a high warming scenario. This scenario is not assigned a likelihood but rather represents a plausible high-risk scenario (Terando et al. 2020).

All of the analyses shown use a reference period of 31 years, spanning from 1980 to 2010. For future analysis, we chose two periods: The midcentury (2030–60) period was chosen to be actionable for decision-makers in fire management (Cullen et al. 2023), and the end-of-the-century (2069–99) period was

TABLE 1. List of simulations used to calculate fire indices. A single ensemble member was used for each RCM–GCM pair, and all outputs were interpolated to a common $^{1}/_{4}^{\circ}$ grid.

GCM	RCM	Grid spacing (°)
GFDL-ESM2M	RegCM4	1/4
GFDL-ESM2M	WRF	1/4
HadGEM2-ES	RegCM4	1/4
HadGEM2-ES	WRF	1/4
MPI-ESM-LR	RegCM4	1/4
MPI-ESM-LR	WRF	1/4
MPI-ESM-LR	CRCM5-UQAM	1/4
MPI-ESM-MR	CRCM5-UQAM	1/4
CanESM2	CRCM5-UQAM	1/4
CanESM2	CanRCM4	1/4
CanESM2	RCA4	1/2
EC-EARTH	RCA4	1/2
EC-EARTH	HIRHAM5	1/2

chosen to examine trends and observe the impacts of extreme climate change. During the midcentury period, the high-end and midrange RCP scenarios (e.g., RCP4.5 and RCP8.5) have not vet diverged significantly, and uncertainty is dominated by internal variability and structural uncertainty stemming from an incomplete knowledge of complex systems, resulting in models having different responses to similar climate forcings. Applying an ensemble of simulations facilitates exploration of the range of potential outcomes (Hawkins and Sutton 2009; Terando et al. 2020). The GCMs used in the NA-COR-DEX simulation ensemble span the equilibrium climate sensitivity of CMIP5 (Bukovsky and Mearns 2020), which makes the ensemble suitable for informing decision-making in the midcentury period. At the end of the century, the scenarios diverge significantly, and uncertainty is dominated by choice of scenario. As NA-CORDEX does not have a comparable simulation ensemble in number of simulations or spread in GCM climate sensitivity for RCP4.5, we constrained our focus to RCP8.5 experiments, which limits the resultant outputs to inform decision-makers about scenario uncertainties (Terando et al. 2020).

GCM and RCM simulations contain systematic biases that can affect the results of fire index calculations. To address the bias in the RCM simulations, we used data that were bias corrected over CONUS against the gridMET observation-based dataset (Abatzoglou 2013) using the N-dimensional multivariate bias correction (mBCN) algorithm method described in Cannon (2018) (McGinnis and Mearns 2021). The reference period used in the bias-correction process of the simulations is 1980–2010, which aligns with the reference period used in our analysis, ensuring that the reference period best reflects real-world conditions.

c. Fire indices

Eight indices related to fire weather are calculated and compared. They are listed in Table 2. The daily variables used in the calculation of fire indices include precipitation (pr), minimum and maximum near-surface air temperature and relative humidity (tmin and tmax, and rhmin and rhmax, respectively), near-surface wind speed (sfcWind), near-surface

relative humidity (hurs), near-surface specific humidity (huss), and surface downwelling shortwave radiation (rsds). The inputs to each index are summarized in Fig. 1. The code used to calculate the fire indices is available to the public (Kessenich and McGinnis 2024), and the input data are available in the NA-CORDEX archive (Mearns et al. 2017).

A major factor in fire ignition and spread is the local topography, soil, and fuels, which vary on a spatial scale far smaller than a 25-km grid. Fuel is only a variable input into energy release component (ERC) and burning index (BI) [which transfers into severe fire danger index (SFDI)], while the rest either address a certain fuel diameter (FM100 and FM1000) or have a single fuel scenario [Canadian Forest Fire Weather Index (CFWI), Keetch-Byram drought index (KBDI), modified Fosberg fire weather index (mFFWI)]. KBDI assumes that 8 in. of moisture can be held in the soil and surface duff (i.e., plant litter) beyond the wilting point, and the wilting point is based on mean annual rainfall (Keetch and Byram 1968). CFWI models a mature pine stand with several static levels of litter and duff fuels (Stocks et al. 1989). Multiple fuel models exist for the NFDRS indices for different vegetation types and are inputs for ERC, BI, and (indirectly) SFDI, so we used two different fuel modeling approaches to examine how fuel modeling affects the results. The first approach models a dense conifer stand with heavy fuel buildup, should produce the most dramatic fire behavior, and is known as fuel model G in the NFDRS system. The second fuel modeling approach, vegetation mosaic (VM), applies a variety of NFDRS fuel models approximating the spatial distribution of fuels across CONUS. While fuel model G has been used extensively in operations, the VM fuel modeling approach is more representative of fuel effects across the domain, which is why both are included in this analysis. The VM approach includes less dramatic fire behavior in response to fuel load and excludes any areas not subject to wildland fire, such as dominantly agricultural areas. Fuels vary greatly within each 1/4° or 1/2° model grid cell, so the largest area fraction method was applied to select a single fuel model for each grid cell from a finer-scale map provided by the Wildland Fire Assessment Program (Burgan et al. 1998). These two fuel modeling approaches are labeled in the results as either ERC/BI/SFDI G or ERC/BI/SFDI VM. In both cases, it is assumed that fuel type is static across time, matching the methodology for landuse/land-cover type used in the climate simulations. The fuel modeling scenarios used to calculate ERC and BI are propagated through to SFDI, as ERC and BI are input into SFDI. As fuels vary on a fine scale, so must fuel treatment, which can aid in managing the risk of fire impact (Prichard et al. 2021). Due to the scale of the projections, fuel treatment is not addressed in this paper, and it is assumed that fuel is present according to the fuel models used in the fire indices.

The fire index calculations required some modification for use with the existing RCM data. Specifically, 1200 local standard time (LST) measurements were substituted with tmax, sfcWind, and rhmin in CFWI, and tmax, tmin, rhmax, and rhmin were substituted for 1300 LST observations in ERC and BI. These substitutions may affect the absolute values of the fire indices such that they are not directly comparable to

TABLE 2. Summary of fire indices.

	Fire				
Fire index name	index acronym	What the fire index indicates	Input variables	Notes	Citations
Keetch–Byram drought index	KBDI	Cumulative moisture deficiency in soil	tmax, prec	Bounded from 0 to 800 where 0 indicates saturated soil and 800 represents severe drought	Keetch and Byram (1968), Alexander (1990)
Modified Fosberg fire weather index	mFFWI	Potential effect of weather conditions on wildland fire	tmax, hurs, sfcWind, KBDI	Open-ended scale	Goodrick (2002)
Canadian Forest Fire Weather Index	CFWI	Potential frontal fire intensity	tmax, rhmin, prec, sfcWind	From the Canadian Forest Fire Weather System. It has an open-ended scale	Stocks et al. (1989)
100-h fuel moisture	FM100	Moisture content of dead fuels that are 1–3 in. in diameter	tmax, tmin, prec, rhmin, rhmax	From the U.S. NFDRS. Higher values indicate more moisture, and low values indicate less moisture, so lower fuel moisture values are associated with higher fire danger, which is opposite to the other fire indices here	Schlobohm and Brain (2002)
1000-h fuel moisture	FM1000	Moisture content in dead fuels that are 3–8 in. in diameter	tmax, tmin, prec, rhmin, rhmax	From the NFDRS. Higher values indicate more moisture, and low values indicate less moisture, so lower fuel moisture values are associated with higher fire danger, which is opposite to the other fire indices here	
Energy release component	ERC	Available energy per unit area within the flaming front at the head of a fire	tmax, tmin, prec, rhmin, rhmax, huss, rsds, FM100, FM1000	From the NFDRS. Open ended and designed to represent the worst-case scenario. Two fuel modeling approaches are applied (G and VM)	
Burning index	BI	Contribution of fire behavior to the effort of containing a fire by combining intensity and spread	tmax, tmin, prec, rhmin, rhmax, huss, rsds, sfcWind, FM100, FM1000, ERC	From the NFDRS. Open ended and designed to represent the worst-case scenario. Two fuel modeling approaches are applied (G and VM)	
Severe fire danger index	SFDI	Normalization of fire danger across space derived from BI and ERC	ERC, BI	Derived from the NFDRS. Five classes of fire danger: low (0–60), moderate (60–80), high (80–90), very high (90–97), and severe (97–100). Two fuel modeling approaches are applied (G and VM)	Jolly et al. (2019)

index values calculated using the original time-based measurements (e.g., tmax may overestimate, or sfcWind may underestimate, conditions at 1200 LST or 1300 LST) (Van Vliet et al. 2024), although such substitutions are less consequential when applied systematically across time as done here.

The indices are calculated daily and continuously for the entire simulation period (1950–2099), regardless of season. Some indices (e.g., CFWI) are operationally only calculated during part of the year, but we calculate all indices year-round and with appropriate spinup time for time-lagged variables (e.g., drought code), to allow for changes in fire weather to occur at any time of year under future conditions.

Fire indices were developed with the expectation that localized expertise would be applied when interpreting their values, and since different indices were developed for different regions, indices should be expected to have varied interpretations across CONUS. From its conception, all the components of the NFDRS system were intended to be subject to local interpretation, with

its default thresholds only recommended in areas where more localized knowledge is unavailable or study has yet to be performed [National Interagency Fire Center (NIFC) 2022]. Applying locally calculated percentile thresholds provides a way to uniformly interpret the indices across space while allowing for different behavior from the indices across space. Unlike the rest of the indices used, SFDI was developed to be interpreted uniformly across space (Jolly et al. 2019). SFDI is built off of percentile thresholds, which is the same as the analyses presented here, but does not eliminate the qualification that not all fire indices should be relied upon equally across CONUS. However, for the sake of completeness, all the fire indices are presented across the entire domain.

d. Methods

1) FIRE DANGER THRESHOLDS

In this paper, we look at future projections of fire danger days by counting daily occurrences of fire index values

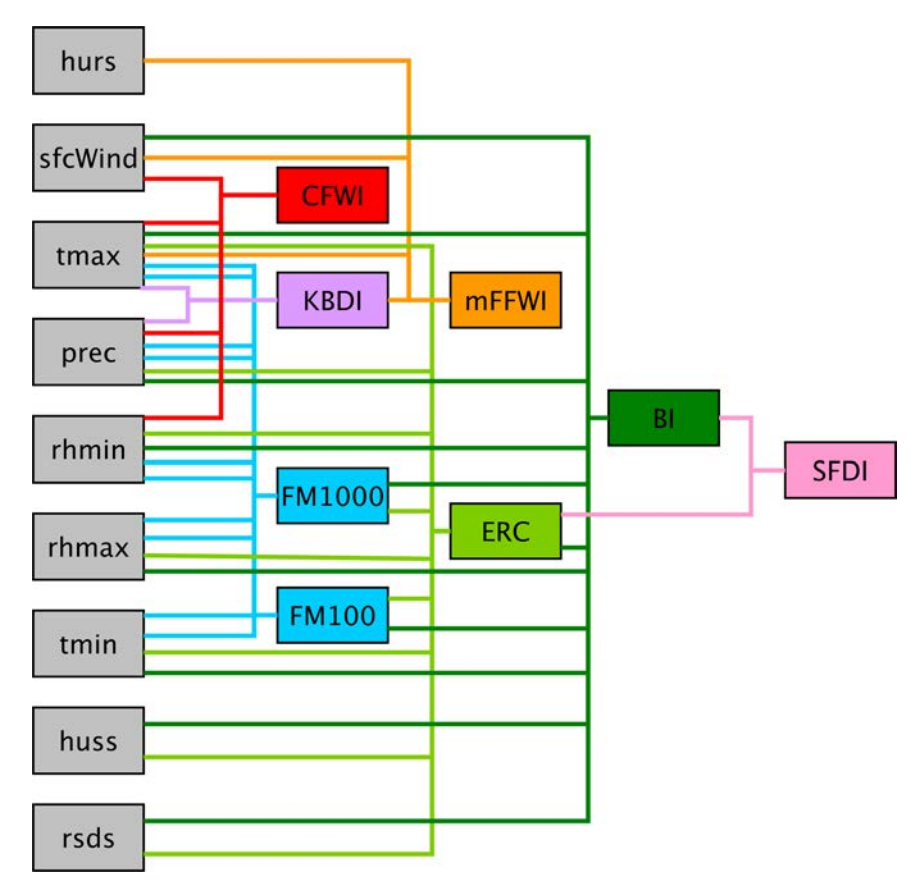


FIG. 1. Flowchart showing the variable inputs into the fire indices. Meteorological variables are in gray rectangles, and each fire index is color coded so that all edges connecting an input to a fire index match the index. FM100 and FM1000 use the same set of inputs and thus are the same color. Variables used as inputs have edges on the right side of the rectangle, and the fire index receives inputs on the left side of the rectangle. The fire indices are arranged in four columns based on the dependencies of the inputs. The indices in the left-most column use only meteorological inputs, the column immediately to its right uses meteorological inputs and fire indices that use only meteorological variables, and so on.

exceeding specific percentile thresholds. These counts are primarily examined as annual sums, which are then averaged for the reference and future time periods to examine change. The percentile thresholds are calculated on a gridcell-by-gridcell basis. Because the interpretation of fire index values varies by the index and due to differences in fuels, climatology, and topography, using percentiles allows us to apply a uniform interpretation across space and index. Percentile thresholds are commonly used to examine changes in fire extremes (e.g., Williams et al. 2019; Abatzoglou and Kolden 2013; Jain et al. 2017; Fox-Hughes et al. 2014; Bedia et al. 2014; Brown et al. 2021), mostly between the 90th and 99th percentiles.

We selected thresholds of the 80th, 90th, and 97th percentile for the entire year based on default thresholds used to assign adjective descriptors of fire danger in the NFDRS system (Schlobohm and Brain 2002, NIFC 2022), the same thresholds and descriptors used for SFDI. "High fire danger days" are those with an index value above the 80th percentile, "very high" are above the 90th percentile, and "severe" are above

the 97th percentile (for FM100 and FM1000, which measure fuel moisture content, lower index values correspond to higher fire danger, and so in this case, high/very high/severe fire danger days are instead those with values below the 20th/10th/3rd percentiles). Heightened fire activity correlates to higher fire danger index values. According to the adjective ratings, "high" corresponds to conditions where "fires may become serious and their control difficult unless they are attacked successfully while small," very high corresponds to conditions where "fires start easily . . . spread rapidly and increase quickly in intensity," and "extreme" corresponds to conditions where "direct attack is rarely possible and may be dangerous except immediately after ignition" (Schlobohm and Brain 2002).

In addition, to examine fire season length, we count the annual number of days above the midpoint value [defined as midpoint = (maximum fire index value + minimum fire index value)/2] from existing methodology in Jolly et al. (2015). This methodology can apply a similar definition of fire season across a range of fire indices, and the midpoint was found to best capture daily

fire activity globally (Jolly et al. 2015). The minimum and maximum values are calculated from the period of 1980–2010.

3) CALCULATION OF FIRE SEASONALITY

Additionally, we examine when high fire danger days occur throughout the year to further explore fire seasonality and whether the timing of fire danger changes in the future. Many papers examine fire weather during a fixed portion of the year (e.g., Tang et al. 2015; Lu et al. 2011; Bedia et al. 2014). Other papers apply dynamic definitions of fire season, which are more localized (e.g., Flannigan et al. 2013; Jain et al. 2017; Fox-Hughes et al. 2014), or a statistical definition of fire season applied to fire indices (e.g., Jolly et al. 2015). Across CONUS, fire season definitions vary within wildland fire management (Cullen et al. 2023). By applying statistical definitions, we can examine shifts in seasonality of fire potential including periods where fire is not historically observed. Our analysis of fire seasonality uses the 80th percentile threshold from the annual analysis but counts biweekly exceedance of the threshold and is spatially averaged across Geographic Area Coordination Centers (GACCs) (NIFC 2022, p. 386). For each RCM, days above the threshold are counted on a gridcell basis, generating a continuous biweekly time series for each point, all of which are then spatially averaged over the GACC, summarized in Fig. 2. GACCs are used to coordinate incident management and resource deployment, and analyzing fire season by GACC can inform practitioners of changes that would affect management practices. This analysis provides additional information that is not captured in annual counts, such as when in the year changes are occurring, differing seasonal behavior between indices, and changes that cancel out when summed.

4) MODEL EVALUATION METHOD

To assess the historical accuracy of the fire index data derived from bias-corrected simulations, we compared the model reference period percentile thresholds against grid-MET. We compared the model ensemble and gridMET on a regional basis using GACCs. Overall, the spatial standard deviation and average spatial thresholds of the percentiles agree between gridMET and the simulation ensemble. Most indices show a less than 5% discrepancy in the average threshold values, with KBDI as a notable exception with discrepancies between 10% and 30%. Scatterplots of this analysis are provided in the supplemental material (Figs. S1–S3 in the online supplemental material) as well as a summary table (Table S1).

5) ENSEMBLE AVERAGING METHODOLOGY

To facilitate the creation of ensemble averages, the simulations with a $^{1}/_{2}^{\circ}$ grid spacing were bilinearly interpolated to the $^{1}/_{4}^{\circ}$ grid spacing of the finer-resolution simulations. Additionally, these ensemble-mean results are presented with a measure of simulation ensemble agreement. The percent of simulations in agreement is scaled/adjusted to account for the possibility of agreement by chance using the Kappa statistic (Bukovsky et al. 2017). We also include the statistical significance of the projected changes in most analyses. Statistical

significance was calculated using a two-sided bootstrapping test at the 0.05 significance level with a bootstrapping sample size of 5000. Similar results were also achieved using a two-sided t test at the 0.1 significance level.

3. Results

We present projections of simulation ensemble agreement for the fire index ensemble to examine high, very high, and severe fire danger days for the midcentury, as well as end-of-the-century results for high fire danger days. A similar analysis is done for days above the midpoint threshold, to examine season length. All thresholds values are plotted in Fig. S5. Across all four thresholds used, the color bar range in Figs. 2–5 remains consistent to facilitate comparison of projected changes. We then examine fire seasonality changes by GACC.

a. High fire danger: Annual count exceeding the historical 80th percentile

We define high fire danger to be fire index values exceeding the historical 80th (for FM100 and FM1000, falling below the 20th) percentile. The simulations project increases in the annual count of high fire danger days across many areas of CO-NUS by midcentury (Fig. 3), though the magnitude of change and degree of model ensemble agreement varies by location and fire index. Across CONUS, KBDI increases are both significant and have high levels of agreement across the ensemble which indicates increases in soil moisture deficit. KBDI shows greater than 80% agreement that the count of high fire danger days will increase by 1-2 months, which is a statistically significant change. Aside from KBDI, CFWI displays the most widespread and statistically significant change across CONUS with high ensemble agreement indicating increased fire intensity. Areas of statistical significance indicate that the change in annual count is outside of the range anticipated by natural interannual variability. In comparison, mFFWI projects fewer areas of statistically significant change than KBDI or CFWI, which suggests the synthesized potential weather effects on fire to be less certain.

The indices within and derived from the NFDRS (FM100, FM1000, ERC, BI, and SFDI) show similar changes in spatial patterns in the count of high fire danger days. As these indices are dependent (Fig. 1), similar patterns emerge in all of them. Both FM100 and FM1000, indicators of fuel moisture, show statistically significant increases in the annual count of high fire danger days in western Montana, southern Oregon, the Southwest, and south-central United States. The increase in count of low fuel moisture days carries over into the spatial distribution of increased days of high fire intensity in ERC as FM100 and FM1000 are inputs into ERC. However, in most areas, ERC shows a smaller magnitude of change in the count of high fire danger days than FM100 and FM1000, and areas of statistically significant change are much smaller. BI uses ERC and also shares similar spatial patterns of change and statistical significance which indicates areas of more extreme fire behavior and spread. SFDI is a combination of BI and ERC, synthesizing spread and intensity into fire danger and shows a balance of the spatial patterns in both. For BI, ERC,

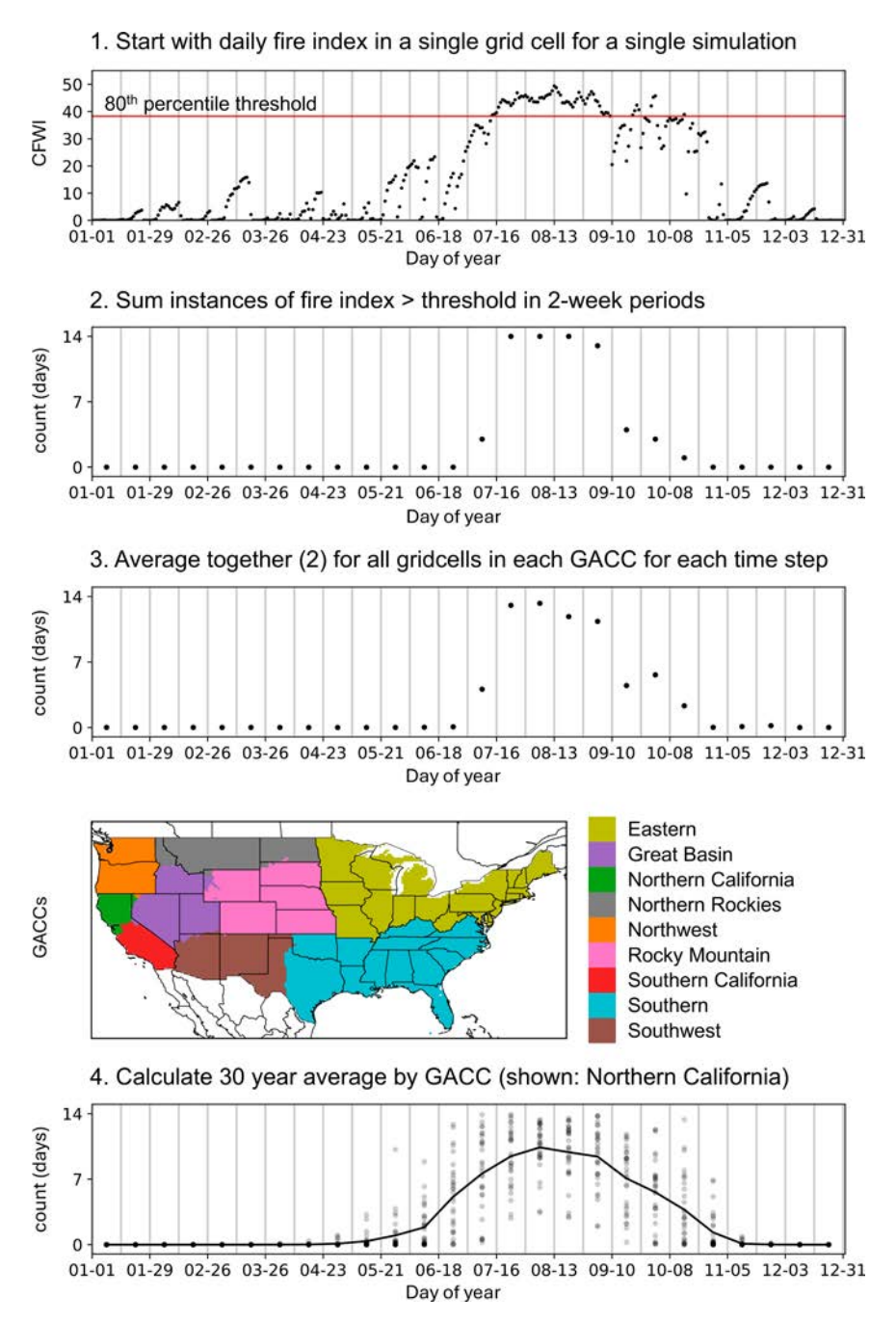


FIG. 2. Calculation steps for fire seasonality by GACC, demonstrated for CFWI calculated from gridMET data in Northern California.

and SFDI, the VM fuel modeling approach projects more pronounced and widespread areas of lower counts of high fire danger days, suggesting that fuel availability does affect the sign of future change. There is strong agreement across the fire index ensemble for significant increases in the count of high fire danger days in southern Texas. In addition, the majority of the fire index ensemble in more than half of the model ensemble projects significant increases in the number of high fire danger days in the Northwest.

All fire indices except for mFFWI use precipitation as a direct input, and changes in precipitation patterns are reflected in the changes in fire indices. Similar plots of significance and change for the fire indices across the model ensemble were made for precipitation projections (Fig. S4). Overall, areas of increased precipitation align with areas of lower model agreement or decreases in the count of high fire danger days. In particular, seasonally relevant increases in precipitation in the Great Basin, Florida, and northern plains align with areas of

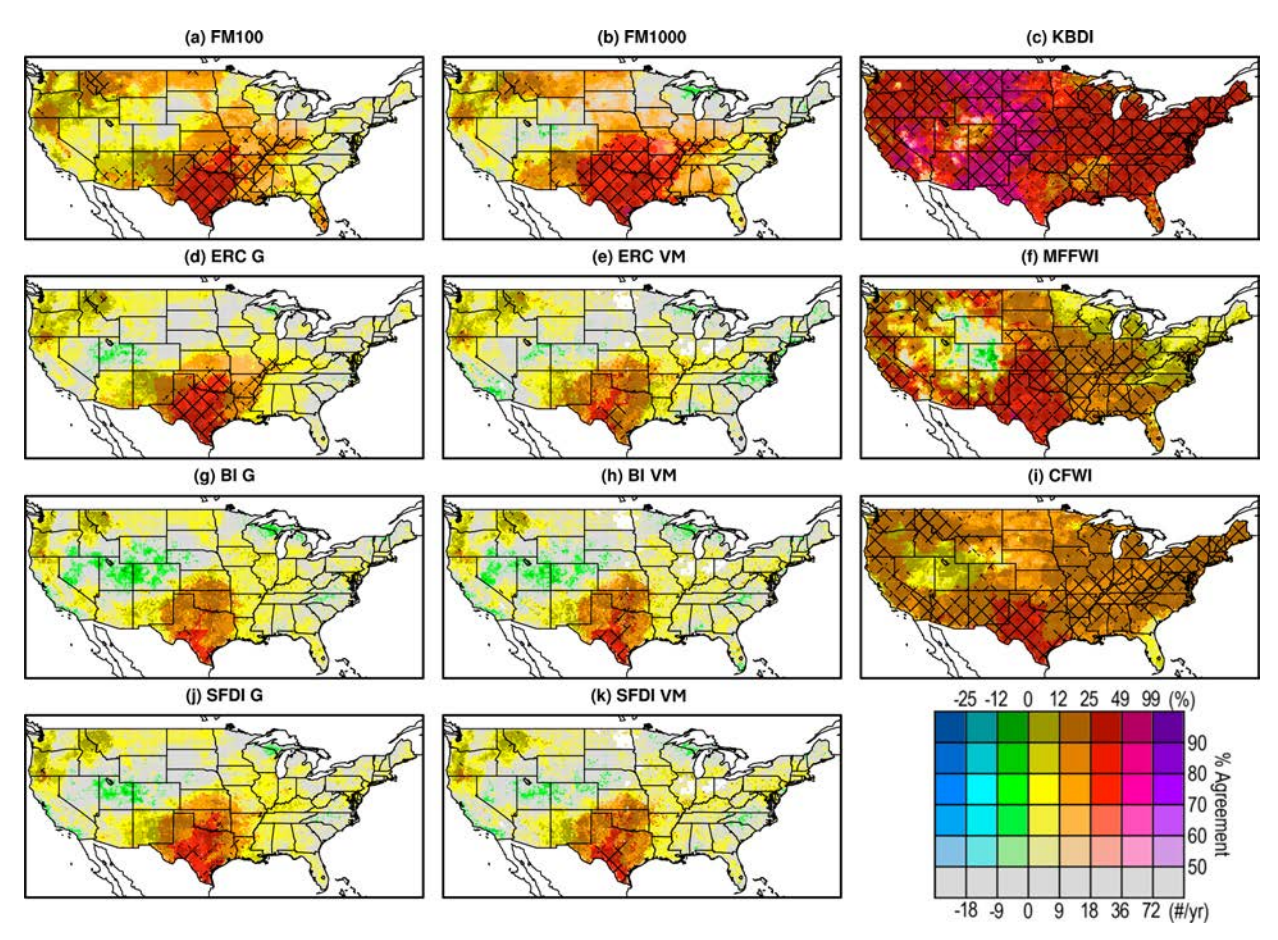


FIG. 3. Change in the annual average number of days above the 80th percentile threshold (below the 20th percentile for FM100 and FM1000) from the baseline period (1980–2010) to midcentury (2030–60). Hatching indicates where the number of simulations projecting a statistically significant change is greater than or equal to 50% of the ensemble, and the number of models agreeing on the sign of change is greater than or equal to 70%. Color indicates that at least half the models agree on the sign of change; areas of disagreement are shaded in gray. The intensity of the color, the color bar y axis, indicates the level of agreement in the ensemble. In the reference period, 73 days are spent above the 80th percentile. The final number of simulations needed for a given range of ensemble agreement is as follows: 90% - 100%, 12-13; 80% - 89%, 11; 70% - 79%, 10; 60% - 69%, 9; 50% - 59%, 8; and less than 50%, 0-7.

lower model agreement, while in Colorado and Utah, increased precipitation in spring and summer aligns with areas of decrease in the length in fire season. The simulations and fire indices disagree on the sign of change in count of high fire danger days in the Rocky Mountains in midcentury, which could also be influenced by increases in projected precipitation interacting with changes in other key variables, such as temperature. In the Northwest, an increase in annual precipitation exists simultaneously with increased high fire danger day counts, as precipitation increases are concentrated in winter and spring, while high fire danger days increase during the summer and fall.

By the end of the century, defined as 2069–99, increases in the count of high fire danger days are larger in magnitude and more widespread than in the midcentury period, as are levels of agreement and statistical significance. For example, KBDI, FM100, and CFWI display increases in the count of high fire danger days of up to 2 months across all of CONUS (Fig. 4).

The ensemble average annual count of high fire danger days at the mid- and end of the century can be found in Figs. S9 and S10 which display all values across the domain, including areas which disagree on the sign of change.

b. Very high and extreme fire danger: Annual count of days exceeding the historical 90th and 97th percentiles

The 90th and 97th percentiles are thresholds of very high and severe fire danger, respectively, and as such, change in the average annual count of days above these thresholds reflects change in the most extreme conditions during fire season. The spatial patterns of change seen in these extremes (Figs. 5 and 6) are similar to the 80th percentile but differ spatially with regard to where statistically significant change is found and the magnitude of that change. For instance, the area of statistically significant change in the Northwest expands in size as the thresholds increase for all NFDRS-associated indices, suggesting fire intensity,

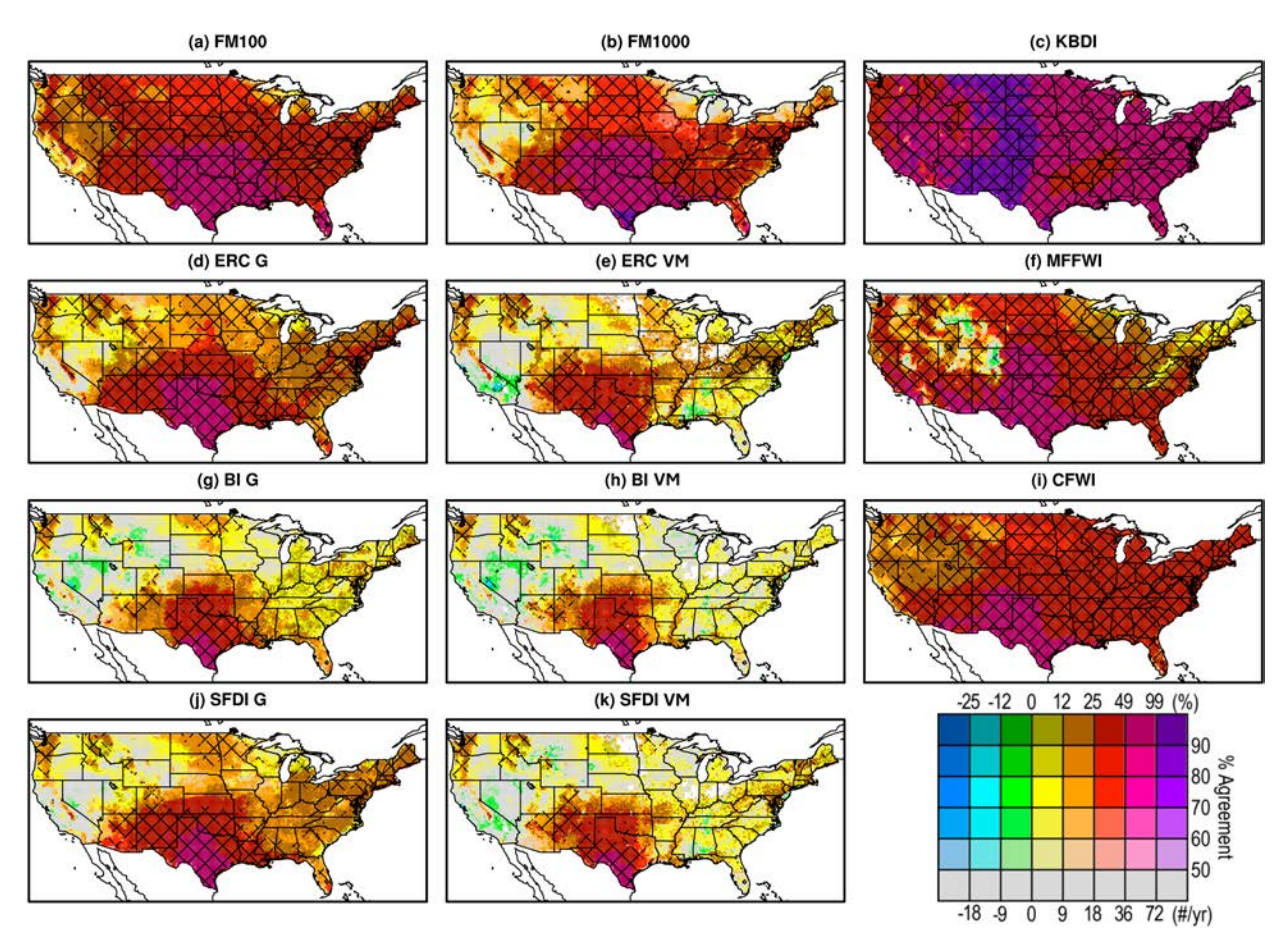


FIG. 4. Change in the annual average number of days above the 80th percentile threshold (below the 20th percentile for FM100 and FM1000) from the baseline period (1980–2010) to end of the century (2069–99). Refer to Fig. 3 for full description.

fire spread, and fuel moisture all contribute to very high fire danger. In Montana and the Idaho Panhandle, FM1000 projects that the area of agreement and statistical significance will expand for the 90th and 97th percentile counts as compared to the 80th percentile, indicating extreme decreases in fuel moisture. Areas of statistical significance do not change spatially for KBDI, but mFFWI and CFWI exhibit a larger area of statistically significant change in the counts above the 90th and 97th percentile thresholds than in the 80th percentile, which suggests larger changes in extreme atmospheric conditions and fire intensity, respectively, compared to the high fire danger percentile. The magnitude of absolute change in the annual count of days above the 90th and 97th percentile tends to be smaller than the count above the 80th percentile, but the percent increase is either similar or larger for all the indices derived from the NFDRS. KBDI shows a similar amount of change across the 80th, 90th, and 97th percentile, and a similar pattern occurs in CFWI in the 80th and 90th percentile counts.

Compared to the count above the 80th percentile, areas projecting a decrease in the count above the 90th and 97th percentiles grow larger and exhibit more model ensemble agreement for NFDRS-associated indices along the East Coast. The same applies to eastern Colorado for BI G, while the opposite is true for eastern Colorado for mFFWI.

For the 90th and 97th percentile counts, change by the end of the century aligns with the patterns seen in the change of annual count above the 80th percentile (Fig. 4 and Figs. S7 and S8). Notably, by the end of the century, most of CONUS experiences significant change in the count of very high and extreme fire danger days according to FM100, FM1000, ERC, and SFDI. However, there still exist areas where the simulations disagree on the sign of change for annual count. Additional areas of low simulation agreement exist in BI, some of which is also seen in SFDI. The rest of the domain experiences significant change in annual count above the extreme thresholds according to BI, which is a far greater area than in the midcentury. By midcentury, KBDI, CFWI, and mFFWI already show statistically significant change across most of CONUS, but most changes double in size from midcentury to the end of the century for these three indices.

Changes in KBDI, shown in red in the 97th percentile, represent at least a 36-day increase over the count of days in the reference period, which is 11 days. Change by the end of the century shown in purple for KBDI shows an increase of 72 days. While these are the most extreme changes in the fire index ensemble, large changes exhibited across the domain should be recognized for their magnitude relative to the reference period. Areas

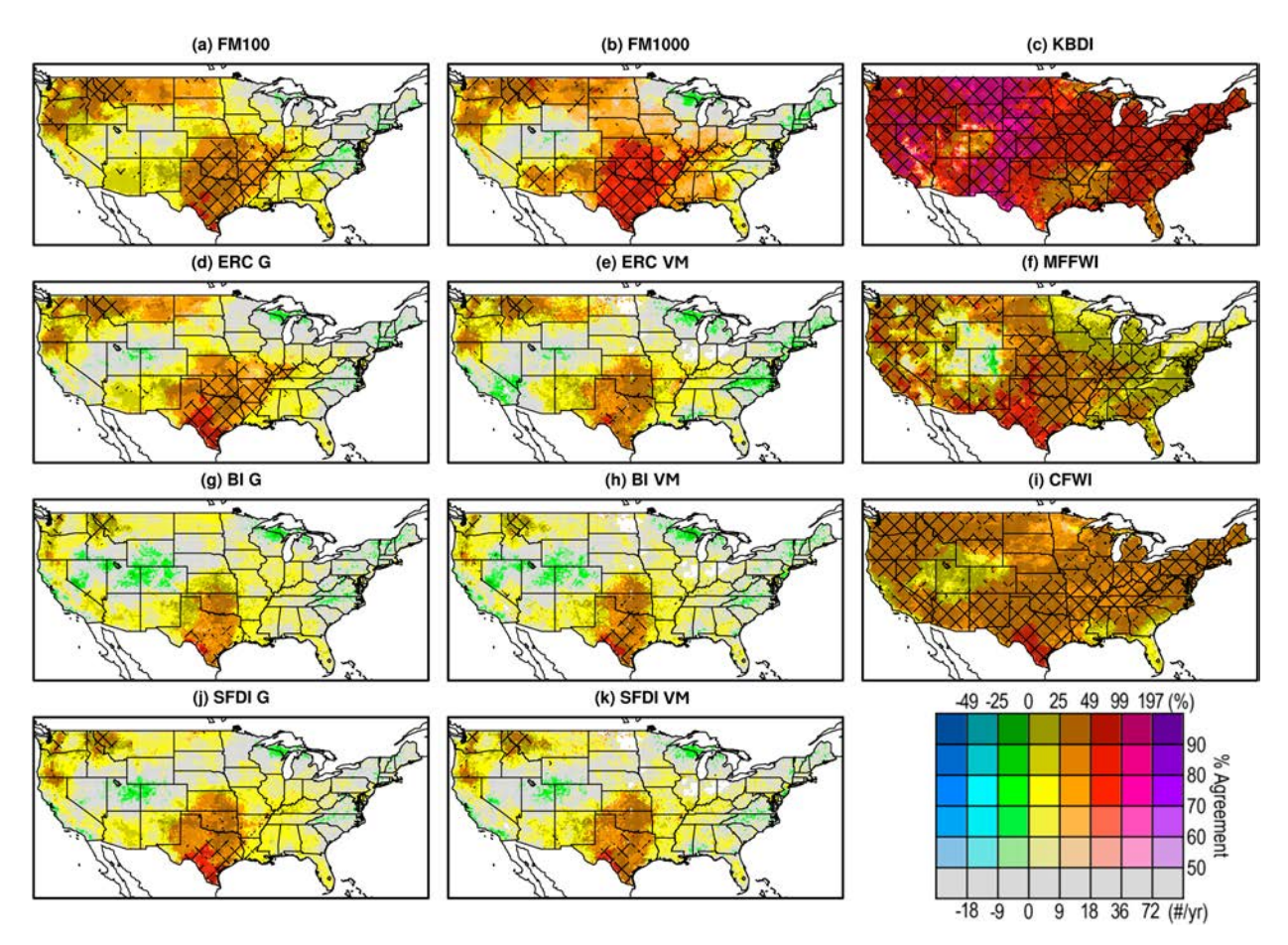


FIG. 5. For the ensemble of fire indices, the change in the annual average number of days above the 90th percentile threshold (below the 10th percentile threshold for FM100 and FM1000) from the baseline period to midcentury. In the reference period, 37 days annually are spent above the 90th percentile. Refer to Fig. 3 for full description.

experiencing 9–18 extra days would experience approximately double the duration of severe fire danger (above 97th percentile) levels relative to the reference period.

The ensemble average annual count of very high and extreme fire danger days at the mid- and end of the century can be found in Figs. S11–S14 which display all values across the domain, including areas which disagree on the sign of change.

c. Season length: Annual count of days above the midpoint

The annual count above the midpoint threshold is used as the definition of fire season length. Similar to changes seen in percentile threshold exceedance counts, KBDI exhibits the most widespread, statistically significant changes, the south-central U.S. region experiences statistically significant change across most fire indices, and NFDRS-derived indices share similar spatial patterns. The Rocky Mountains show either areas of disagreement on the sign of change or areas of decreases in the days above the midpoint across most fire indices, with the exception of FM100, which displays statistically significant increases (Fig. 7).

The magnitude of increases in the annual count exceeding the midpoint ranges from 0 to 18 days as seen in ERC, BI, and VM and 36–72 days as seen in KBDI. By the end of the century, the areas experiencing increases in count above the midpoint have expanded in size and have larger areas of statistically significant change (Fig. S6). Additionally, the size of the increases in count is larger in magnitude.

d. Seasonality by GACC

The annual count plots (e.g., Fig. 3) do not capture fire seasonality (i.e., the timing of fire potential throughout the year), obscuring future changes that could still be relevant, such as shifting season windows or peak timing. The distribution of days above a given fire danger index threshold across the year for the reference period shows the timing of expected fire danger peak and intensity, which vary by index and region and represents a basis for comparison for future time periods (Fig. 8).

Distinct seasonal patterns can be seen in the different GACCs in gridMET and the simulation reference period. The NFDRS indices all share very similar patterns. The Northern Rockies, East, Rocky Mountains, and South GACCs all exhibit bimodality. The Southwest GACC has a monomodal season

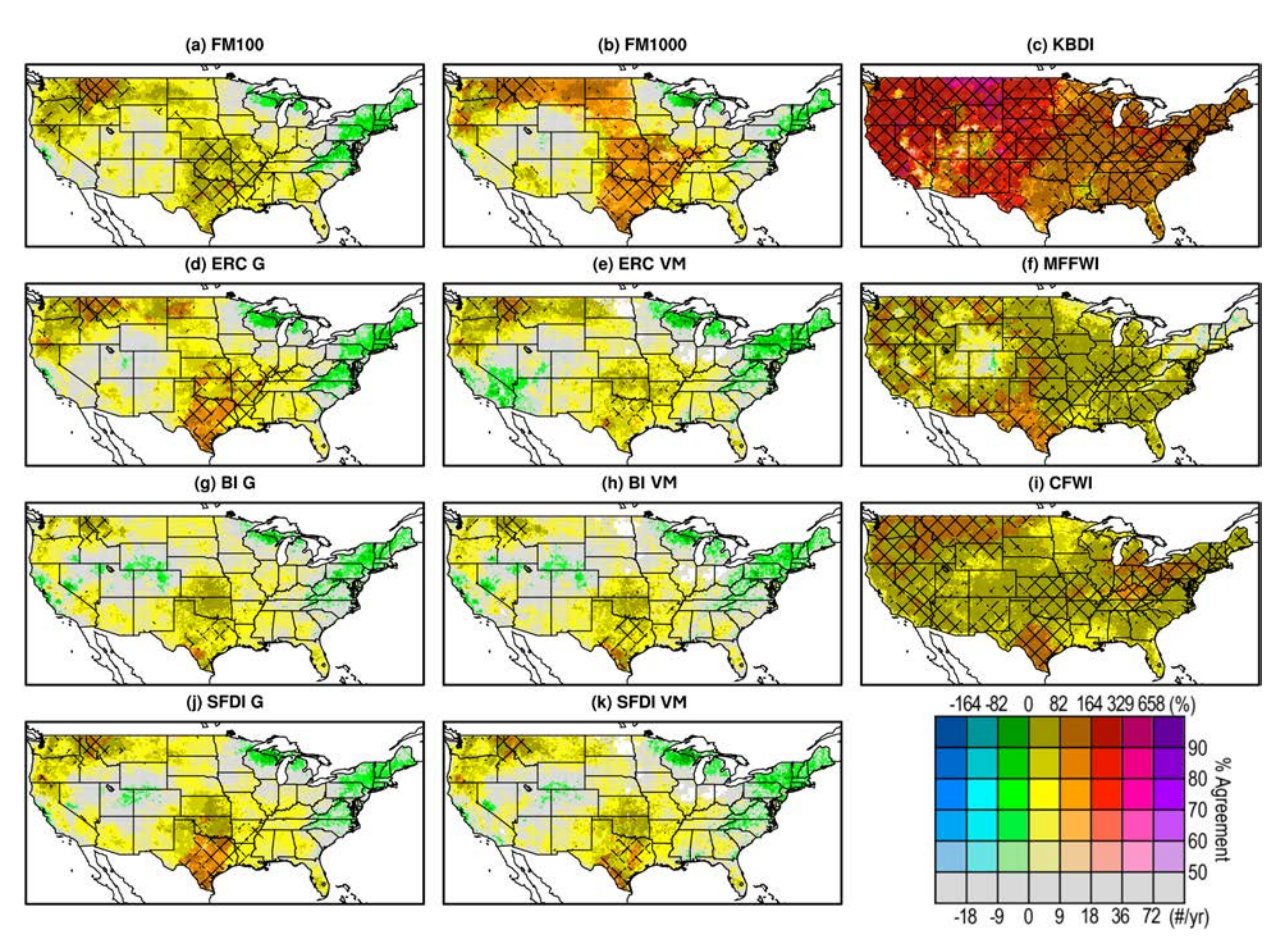


FIG. 6. For the ensemble of fire indices, the change in the annual average number of days above the 97th percentile threshold (below the 3rd percentile threshold for FM100 and FM100) from the baseline period to midcentury. In the reference period, 11 days annually are spent above the 97th percentile. Refer to Fig. 3 for full description.

concentrated in April-June, whereas Northern California, Southern California, Great Basin, and Northwest GACCs have unimodal seasons that peak in July or August. CFWI aligns with the NFDRS indices in the western GACCs but displays a unique seasonality in the South and East GACCs. In contrast, mFFWI mostly agrees with the NFDRS indices in the East, South, and Southwest GACCs, while displaying a unique seasonality in the western GACCs. KBDI has a distinct seasonal pattern that does not align with any other index, peaking later and always having a unimodal season. The seasonal patterns seen in the simulation ensemble and observations gridMET are comparable in most GACCs, but they do not always align. In the Northern Rockies and Rocky Mountain GACCs, grid-MET displays a bimodal seasonal pattern, while the simulation ensemble either captures a monomodal season or a less prominent bimodal pattern. The bimodal season in gridMET is better captured in the South and East GACCs by the simulation ensemble. This should be recognized as a potential limitation of the simulation ensemble.

Season shifts can be seen in several GACCs. For example, by midcentury, FM100 and FM1000 project a later start and a later end of season by 2–4 in the east, Northern Rockies, and

Rocky Mountain GACCs, indicating a shift in when low fuel moisture occurs. This shift is not evident in the annual counts (e.g., Fig. 3). Other indices in the Northwest, as well as in Northern California, South, Southern California, and Southwest, project an expanding season that starts earlier and ends later. This is a change more easily captured by annual counts. KBDI uniquely projects year-round increases in the Rocky Mountains, South, Southern California, and Southwest GACCs indicating constant, heightened deficits in soil moisture. Frequently, ERC, BI, and SFDI project little to no change or are indeterminate. Changes at the end of the century tend to be larger in magnitude and exhibit similar patterns as the midcentury period, but model ensemble disagreement remains high.

The timing of the peak fire season is another characteristic that is not captured by the annual count plots. While most indices and GACCs do not show a shift in the timing of peak fire danger, there are a couple GACCs where a shift is projected. In the Rocky Mountain GACC, the peak occurrence of days above the 80th percentile is projected to shift 2–4 weeks later according to FM100, FM1000, ERC, and CFWI. In the East GACC, the peak occurrence of this count is projected to shift 4–6 weeks later in the year in FM1000, ERC G, and CFWI.

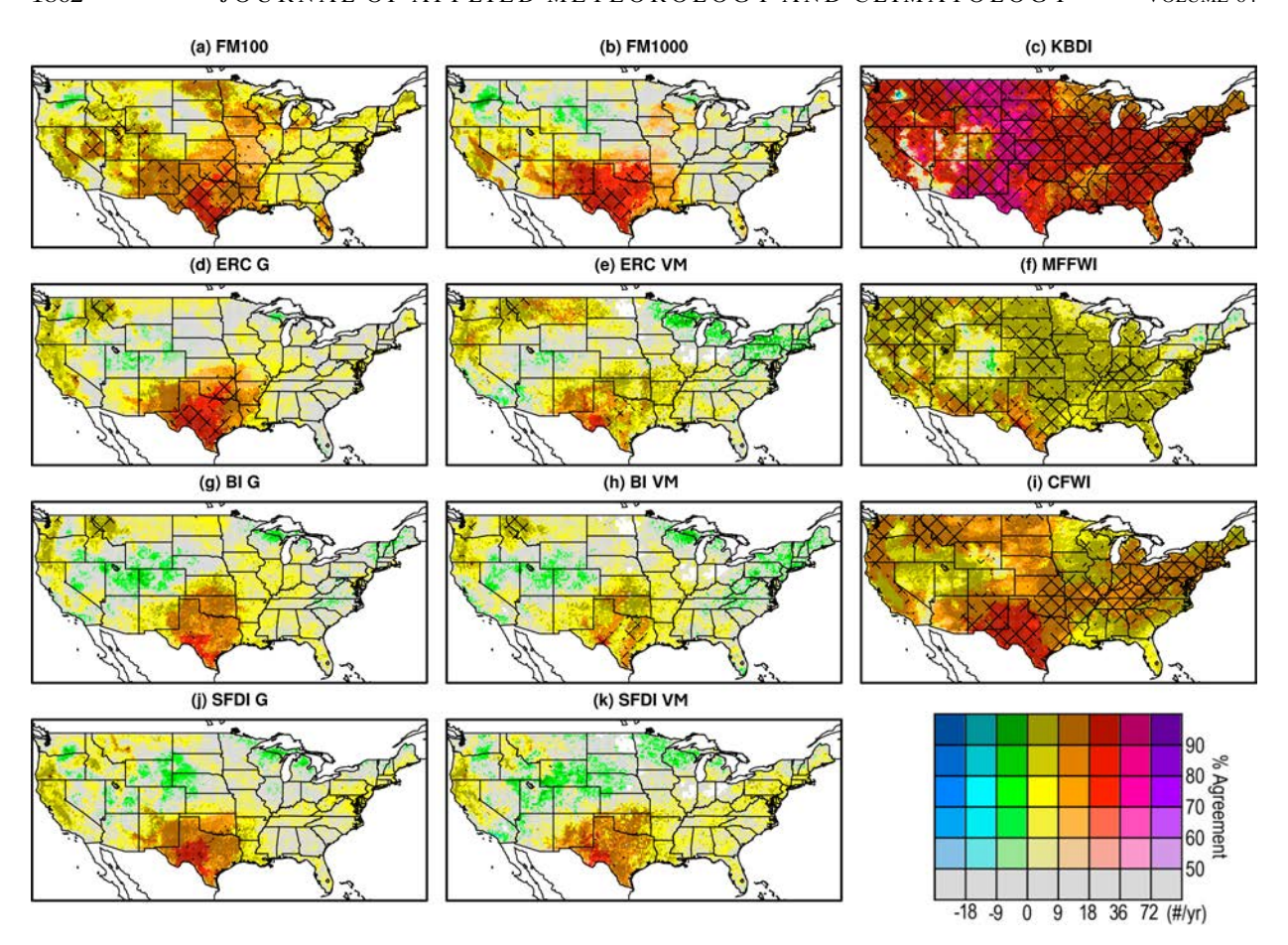


FIG. 7. For the ensemble of fire indices, the change in the annual average number of days above the midpoint threshold from the baseline period to midcentury. Refer to Fig. 3 for full figure interpretation description.

4. Discussion and conclusions

a. Comparing fire indices

Presenting data in familiar frameworks, such as existing fire metrics, can increase usability by practitioners (Cullen et al. 2023). In this work, we focused on metrics that are familiar to practitioners across the United States. Some indices were chosen for their actionability; KBDI, FM100, FM1000, ERC, and BI are all commonly used by fire management in the United States (Melton 1989; Schlobohm and Brain 2002). While less frequently discussed, mFFWI builds off KBDI to incorporate wind and humidity, which are fire-relevant variables beyond drought. CFWI has been adopted by some practitioners in the United States and elsewhere outside Canada (Taylor and Alexander 2006).

The projected changes in the number of days above the examined thresholds in this analysis vary in magnitude and spatial distribution across the fire index ensemble, and projected increases in counts above the examined thresholds are far more widespread and frequently larger than decreases. These results have implications for planning and decision-making, and they demonstrate a limitation of previous research that uses one fire index to examine future fire weather. Some previous analyses

rely solely on KBDI (Brown et al. 2021; Liu et al. 2010). Others rely on CFWI or other components of the Canadian Forest Fire Danger Rating System (CFFDRS) (Goss et al. 2020; Flannigan et al. 2013; Jain et al. 2017). Others still examine the Haines index (Tang et al. 2015) or the MacArthur forest fire danger index (Fox-Hughes et al. 2014), neither of which were examined here. Single indices, applied across a range of ecological conditions or a large domain, often with nonlocalized thresholds of fire danger, have limited applicability. Areas that disagree on the sign of change or exhibit vastly different amounts of change in this analysis indicate areas where the choice of index is critical.

KBDI is an outlier from all other indices examined in this analysis, with changes across the domain that double or quadruple the counts of fire danger days seen in other indices. Large increases in KBDI have been previously attributed to increases in temperature under climate change (Brown et al. 2021). This is likely because KBDI oversimplifies evapotranspiration to be a temperature-driven function, which may not be appropriate across diverse environments and may overestimate the impacts of climate change (Sheffield et al. 2012). Since KBDI is an input into mFFWI, this large temperature-driven increase is carried through to mFFWI. However, mFFWI also uses average daily

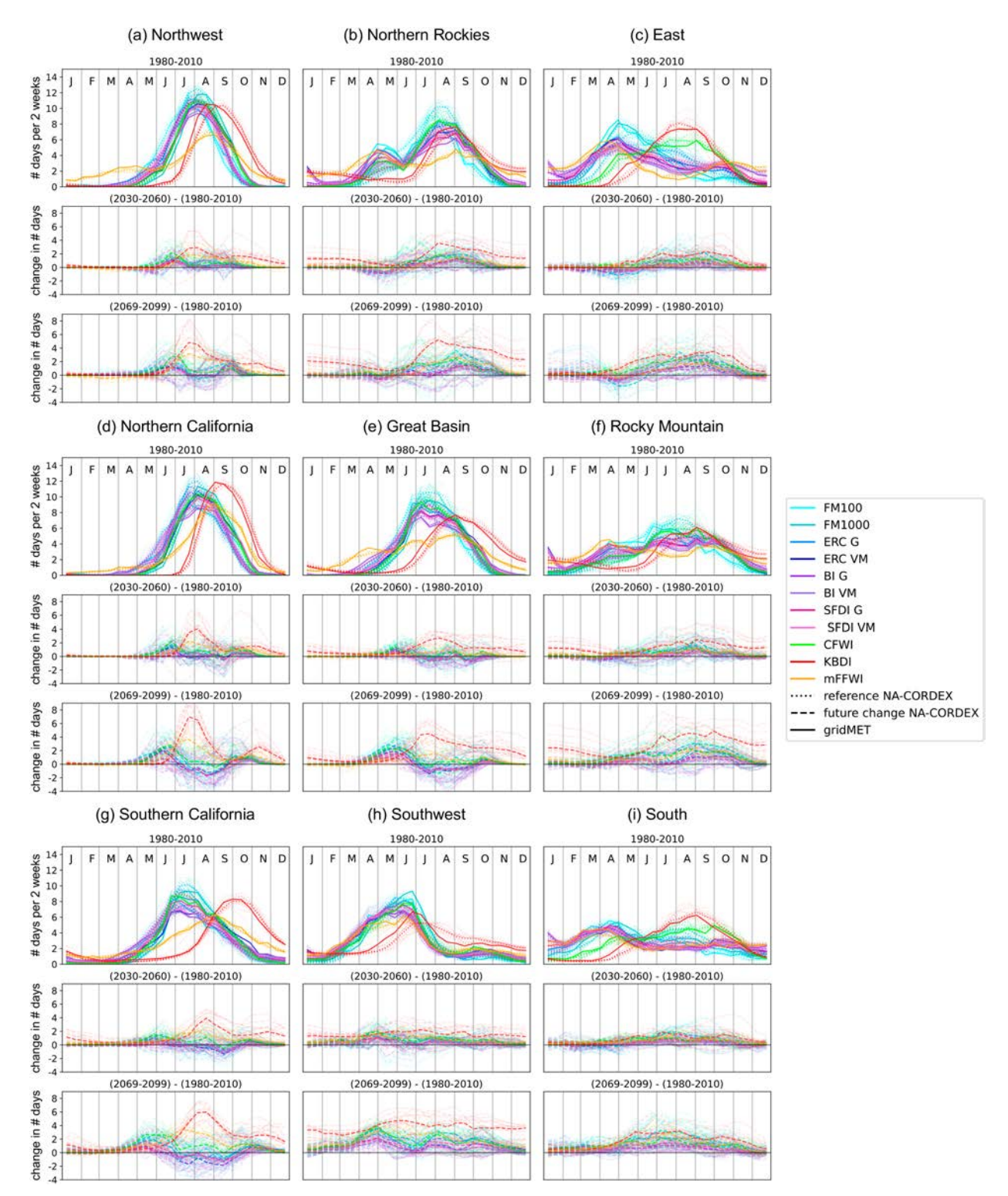


FIG. 8. The 30-yr average of biweekly counts exceeding the 80th percentile threshold for the reference period (colored dotted lines) and gridMET (colored solid lines), change by the midcentury period (colored dashed lines), and change by the end of century period (colored dashed lines). The colors represent fire indices, while the line style represents the source dataset, which are represented in black in the legend. Ensemble medians are shown in bold, while individual simulations are faint.

humidity, which may better reflect future interactions in the fire weather system.

Some NFDRS indices are inputs into other NFDRS indices and share similar spatial patterns of change. NFDRS indices also exhibit far more areas of disagreement on the sign of change than the other indices. ERC and BI are less sensitive to temperature increases, as they place less weight on temperature and place more weight on precipitation (Yu et al. 2023), and there are significant variations across the ensemble in the projected amounts of change in precipitation (Fig. S4).

The simulation ensemble projects large areas of statistically significant change in CFWI, which is independently calculated from all other indices examined here. Previous studies have examined the sensitivity of the CFFDRS system and found that temperature effects dominate precipitation effects (Flannigan et al. 2016).

The subset of indices considering wind (mFFWI, CFWI, BI) exhibits different patterns of change. This suggests that projected wind does not act as a dominant contributor to the average projected changes in fire weather, or the effects of wind as it pertains to dry conditions do not change for the percentile thresholds considered here. This is consistent with Yu et al. (2023), who demonstrated that overall, wind has the least impact of all the inputs for BI and CFWI. However, wind plays a larger role for conditions above the 95th percentile.

Areas of spatial consensus or disagreement that are consistent across the fire index ensemble could point to areas of increased or decreased confidence, respectively, in the change in fire danger. The Rocky Mountains and Great Basin are areas of least consensus in every fire index, so few conclusions can be drawn about increases in fire danger for this examination. In contrast, the Southwest and south-central United States exhibit the most agreement in projected increases in fire danger, increases which are statistically significant in all fire indices except for those using the VM fuel modeling scenario. With slightly less prevalent statistically significant increases but still showing agreement in the sign of change, the Northwest is projected to experience increases in fire danger days across the fire index ensemble. Areas showing more mixed signals across the fire index ensemble include the northern Rockies, which has statistically significant change and high model ensemble agreement in all but ERC, BI, and SFDI (all of which are closely related); California, which has disagreement in NFDRS indices but increases in the non-NFDRS indices; and the east and south, which are projected to experience increases in non-NFDRS indices but decreases according to NFDRS indices.

ERC and BI include fuel loading with live and dead fuels, unlike the other indices examined here, so we examined two fuel modeling scenarios to understand the impacts of fuel model on future projections. In most regions, the choice of fuel model does not change the magnitude of the projected changes. However, the projections of fire weather in the southwest and southcentral United States experience larger magnitude and more widespread statistically significant change under fuel model G than under the mixed fuel model approach, VM. That there are differences in the two indicates that in some regions, like the Southwest, the fuel model chosen as input into the indices does matter and should be considered carefully.

Finally, the different percentile thresholds for fire danger approximate the various NFDRS defined levels of fire danger, and different patterns of change can be seen in the thresholds, varying by region and index. Overall the 97th percentile, approximating severe fire danger experiences smaller absolute change but larger relative change, compared to the other thresholds. The 90th and 97th percentiles exhibit smaller absolute changes than the 80th percentile, but the spatial patterns of statistical significance are consistent across all three.

b. Limitations

The grid spacing of the regional simulations must be considered when using these data. At 25 km or 50 km, each grid cell is 625 or 2500 km² in area. While this is suitable for general climate analysis, this may be difficult to translate to local applications, particularly where terrain or fuel are major influences on fire behavior. Similarly, comparison of the gridded data presented here may not be easily used in tandem with point-based observations of fire indices in complex orography.

The GACC seasonality summaries comparing gridMET to simulations suggest that some atmospheric processes relevant to fire, particularly in the spring, are not being captured in the simulations in a uniform manner.

c. Using fire indices to address future meteorological trends

The input variables for the fire indices project potentially counteracting and/or compounding interactions with each other. Whether the fire indices are able to capture these interactions affects their usability in future fire projections. Increased precipitation dampens fire potential in the fire indices, but higher temperatures drive fuel curing and increases fire potential. Decreases in precipitation and rising temperatures can compound for some regions as well. The NA-CORDEX RCM ensemble exhibits increases in temperature, and precipitation increases or decreases by region and season (Fig. S4). Since fire indices rely heavily on both, the covariability of these changes impacts the projected fire indices. For instance, regions with increased winter and spring precipitation would not experience dampened fire potential in the summer and fall, when projected temperature increases are higher. Increased precipitation would also contribute to fuel growth, but the fire indices do not address fuel growth dynamics, and thus, effects of fuel availability (such as in a fuel-limited regime) are not captured by these projections. Previous studies of the effects of climate change on wildland fire suggest that increased fuel aridity attributed to climate change has already affected the magnitude of area burned by forest fires in recent years (Williams et al. 2019).

How the inputs interact in the fire indices should be considered as well. A study of observations shows that decreased precipitation or precipitation feedbacks through vapor pressure deficit were major drivers behind the increased burn area from 1979 to 2016 (Holden et al. 2018), which would suggest that future increases in fire-season precipitation could prevent that trend from continuing. Indices with many input variables, such as ERC and BI, have the ability to capture complex interactions, but increased fidelity in the input variables is required for

those interactions to be accurate (Yu et al. 2023). Overall, by midcentury, there are many areas of disagreement in this ensemble's projections, but by the end of the century, nonprecipitation variables (i.e., high levels of warming) appear to be driving an increase in dangerous fire weather in direct conflict with increased precipitation.

Future work could include the modeling of ignitions, including human-caused ignitions, in addition to extending this analysis to impacts on human health, safety, and wellbeing.

Acknowledgments. We gratefully acknowledge the National Science Foundation's Growing Convergence Research Program (Award 2019762 "Managing Future Risk of Increasing Simultaneous Megafire") for support of this research. We also acknowledge the U.S. Department of Energy Regional and Global Climate Modeling program Award DOE DE-SC0016605. We acknowledge the World Climate Research Programme's Working Group on Regional Climate and the Working Group on Coupled Modelling, former coordinating body of CORDEX and responsible panel for CMIP5. We also thank the climate modelling groups for producing and making available their model output. We also acknowledge the U.S. Department of Defense Environmental Security Technology Certification Program for its support of the NA-CORDEX data archive. We would like to acknowledge computing support from the Casper system (https://ncar.pub/casper) provided by the NSF National Center for Atmospheric Research (NCAR), sponsored by the National Science Foundation. We also gratefully acknowledge the feedback and thoughtful comments of three anonymous reviewers on the draft of this paper.

Data availability statement. All fire index data created or used during this study are openly available from the NA-CORDEX data archive at https://doi.org/10.5065/D6SJ1JCH. Software for this research is available in in-text data citation references: Kessenich and McGinnis (2024).

REFERENCES

- Abatzoglou, J. T., 2013: Development of gridded surface meteorological data for ecological applications and modelling. *Int. J. Climatol.*, 33, 121–131, https://doi.org/10.1002/joc.3413.
- —, and T. J. Brown, 2012: A comparison of statistical downscaling methods suited for wildfire applications. *Int. J. Climatol.*, 32, 772–780, https://doi.org/10.1002/joc.2312.
- —, and C. A. Kolden, 2013: Relationships between climate and macroscale area burned in the western United States. *Int. J. Wildland Fire*, 22, 1003, https://doi.org/10.1071/WF13019.
- —, and A. P. Williams, 2016: Impact of anthropogenic climate change on wildfire across western US forests. *Proc. Natl. Acad. Sci. USA*, **113**, 11770–11775, https://doi.org/10.1073/ pnas.1607171113.
- Alexander, M. E., 1990: Computer calculation of the Keetch-Byram Drought Index-programmers beware! Fire Manage. Notes, 51, 23–25.
- Baijnath-Rodino, J. A., P. V. V. Le, E. Foufoula-Georgiou, and T. Banerjee, 2023: Historical spatiotemporal changes in fire

- danger potential across biomes. Sci. Total Environ., 870, 161954, https://doi.org/10.1016/j.scitotenv.2023.161954.
- Bedia, J., S. Herrera, A. Camia, J. M. Moreno, and J. M. Gutiérrez, 2014: Forest fire danger projections in the Mediterranean using ENSEMBLES regional climate change scenarios. *Climatic Change*, 122, 185–199, https://doi.org/10.1007/s10584-013-1005-z.
- —, —, J. M. Gutiérrez, A. Benali, S. Brands, B. Mota, and J. M. Moreno, 2015: Global patterns in the sensitivity of burned area to fire-weather: Implications for climate change. *Agric. For. Meteor.*, 214–215, 369–379, https://doi.org/10.1016/ j.agrformet.2015.09.002.
- Black, C., Y. Tesfaigzi, J. A. Bassein, and L. A. Miller, 2017: Wildfire smoke exposure and human health: Significant gaps in research for a growing public health issue. *Environ. Toxicol. Pharmacol.*, 55, 186–195, https://doi.org/10.1016/j.etap.2017.08.022.
- Bradshaw, L. S., J. E. Deeming, R. E. Burgan, and J. D. Cohen, 1983: The 1978 National fire-danger rating system: Technical documentation. USDA Forest Service General Tech. Rep. INT-169, 49 pp.
- Brown, E. K., J. Wang, and Y. Feng, 2021: US wildfire potential: A historical view and future projection using high-resolution climate data. *Environ. Res. Lett.*, 16, 034060, https://doi.org/ 10.1088/1748-9326/aba868.
- Bukovsky, M. S., and L. O. Mearns, 2020: Regional climate change projections from NA-CORDEX and their relation to climate sensitivity. *Climatic Change*, 162, 645–665, https://doi. org/10.1007/s10584-020-02835-x.
- —, R. R. McCrary, A. Seth, and L. O. Mearns, 2017: A mechanistically credible, poleward shift in warm-season precipitation projected for the U.S. southern Great Plains? *J. Climate*, 30, 8275–8298, https://doi.org/10.1175/JCLI-D-16-0316.1.
- Burgan, R., R. Klaver, and J. Klaver, 1998: Fuel models and fire potential from satellite and surface observations. *Int. J. Wildland Fire*, 8, 159, https://doi.org/10.1071/WF9980159.
- Cannon, A. J., 2018: Multivariate quantile mapping bias correction: An *N*-dimensional probability density function transform for climate model simulations of multiple variables. *Climate Dyn.*, **50**, 31–49, https://doi.org/10.1007/s00382-017-3580-6.
- Cullen, A. C., T. Axe, and H. Podschwit, 2021: High-severity wild-fire potential—Associating meteorology, climate, resource demand and wildfire activity with preparedness levels. *Int. J. Wildland Fire*, 30, 30, https://doi.org/10.1071/WF20066.
- —, and Coauthors, 2023: Growing convergence research: Coproducing climate projections to inform proactive decisions for managing simultaneous wildfire risk. *Risk Anal.*, 43, 2262–2279, https://doi.org/10.1111/risa.14113.
- —, B. R. Goldgeier, E. Belval, and J. T. Abatzoglou, 2024: Characterising ignition precursors associated with high levels of deployment of wildland fire personnel. *Int. J. Wildland Fire*, 33, WF23182, https://doi.org/10.1071/WF23182.
- Flannigan, M. D., A. S. Cantin, W. J. De Groot, M. Wotton, A. Newbery, and L. M. Gowman, 2013: Global wildland fire season severity in the 21st century. For. Ecol. Manage., 294, 54–61, https://doi.org/10.1016/j.foreco.2012.10.022.
- —, B. M. Wotton, G. A. Marshall, W. J. De Groot, J. Johnston, N. Jurko, and A. S. Cantin, 2016: Fuel moisture sensitivity to temperature and precipitation: Climate change implications. *Climatic Change*, 134, 59–71, https://doi.org/10.1007/s10584-015-1521-0.
- Fox-Hughes, P., R. Harris, G. Lee, M. Grose, and N. Bindoff, 2014: Future fire danger climatology for Tasmania, Australia, using a dynamically downscaled regional climate model. *Int. J. Wildland Fire*, 23, 309, https://doi.org/10.1071/WF13126.

- Goodrick, S. L., 2002: Modification of the Fosberg fire weather index to include drought. *Int. J. Wildland Fire*, **11**, 205–211, https://doi.org/10.1071/WF02005.
- Goss, M., D. L. Swain, J. T. Abatzoglou, A. Sarhadi, C. A. Kolden, A. P. Williams, and N. S. Diffenbaugh, 2020: Climate change is increasing the likelihood of extreme autumn wildfire conditions across California. *Environ. Res. Lett.*, 15, 094016, https:// doi.org/10.1088/1748-9326/ab83a7.
- Hawkins, E., and R. Sutton, 2009: The potential to narrow uncertainty in regional climate predictions. *Bull. Amer. Meteor. Soc.*, 90, 1095–1108, https://doi.org/10.1175/2009BAMS2607.1.
- Holden, Z. A., and Coauthors, 2018: Decreasing fire season precipitation increased recent western US forest wildfire activity. *Proc. Natl. Acad. Sci. USA*, 115, E8349–E8357, https://doi.org/10.1073/pnas.1802316115.
- Jain, P., X. Wang, and M. D. Flannigan, 2017: Trend analysis of fire season length and extreme fire weather in North America between 1979 and 2015. *Int. J. Wildland Fire*, 26, 1009, https:// doi.org/10.1071/WF17008.
- Jolly, W. M., M. A. Cochrane, P. H. Freeborn, Z. A. Holden, T. J. Brown, G. J. Williamson, and D. M. J. S. Bowman, 2015: Climate-induced variations in global wildfire danger from 1979 to 2013. *Nat. Commun.*, 6, 7537, https://doi.org/10. 1038/ncomms8537.
- —, P. H. Freeborn, W. G. Page, and B. W. Butler, 2019: Severe Fire Danger Index: A forecastable metric to inform firefighter and community wildfire risk management. *Fire*, 2, 47, https://doi.org/10.3390/fire2030047.
- Keetch, J. J, and G. M. Byram, 1968: A drought index for forest fire control. USDA. Forest Service Research Paper SE-38. 33 pp., https://research.fs.usda.gov/treesearch/40.
- Kessenich, L., and S. McGinnis, 2024: NCAR/fire-indices: Fire index collection in NCL, version v1.1.0. Zenodo, https://doi.org/10.5281/ZENODO.13798929.
- Littell, J. S., D. L. Peterson, K. L. Riley, Y. Liu, and C. H. Luce, 2016: A review of the relationships between drought and forest fire in the United States. *Global Change Biol.*, 22, 2353– 2369, https://doi.org/10.1111/gcb.13275.
- Liu, Y., J. Stanturf, and S. Goodrick, 2010: Trends in global wild-fire potential in a changing climate. For. Ecol. Manage., 259, 685–697, https://doi.org/10.1016/j.foreco.2009.09.002.
- Lu, W., J. J. Charney, S. Zhong, X. Bian, and S. Liu, 2011: A North American regional reanalysis climatology of the Haines Index. *Int. J. Wildland Fire*, 20, 91, https://doi.org/10. 1071/WF08196.
- McGinnis, S., and L. Mearns, 2021: Building a climate service for North America based on the NA-CORDEX data archive. *Climate Serv.*, 22, 100233, https://doi.org/10.1016/j.cliser.2021. 100233.
- Mearns, L. O., and Coauthors, 2017: The NA-CORDEX dataset, version 1.0. NCAR Climate Data Gateway, accessed 17 January 2024, https://doi.org/10.5065/D6SJ1JCH.
- Melton, M., 1989: The Keetch/Byram Drought Index: A guide to fire conditions and suppression problems. *Fire Manage. Notes*, **50**, 30–34.
- Moss, R., and Coauthors, 2008: Towards New Scenarios for Analysis of Emissions, Climate Change, Impacts, and Response Strategies. IPCC, 155 pp.
- NIFC, 2022: Interagency standards for fire and fire aviation operations. NFES 2724, 510 pp., https://www.nifc.gov/sites/default/files/redbook/archive/2022RedBook.pdf.
- Podschwit, H., and A. Cullen, 2020: Patterns and trends in simultaneous wildfire activity in the United States from 1984 to

- 2015. Int. J. Wildland Fire, 29, 1057–1071, https://doi.org/10.1071/WF19150.
- Preisler, H. K., S.-C. Chen, F. Fujioka, J. W. Benoit, and A. L. Westerling, 2008: Wildland fire probabilities estimated from weather model-deduced monthly mean fire danger indices. *Int. J. Wildland Fire*, 17, 305, https://doi.org/10.1071/WF06162.
- Prichard, S. J., and Coauthors, 2021: Adapting western North American forests to climate change and wildfires: 10 common questions. *Ecol. Appl.*, 31, e02433, https://doi.org/10.1002/eap. 2433.
- Richardson, D., A. S. Black, D. Irving, R. J. Matear, D. P. Monselesan, J. S. Risbey, D. T. Squire, and C. R. Tozer, 2022: Global increase in wildfire potential from compound fire weather and drought. *npj Climate Atmos. Sci.*, 5, 23, https://doi.org/10.1038/s41612-022-00248-4.
- Schlobohm, P., and J. Brain, 2002: Gaining and understanding of the National Fire Danger Rating System. National Wildfire Coordinating Group, Fire Danger Working Team PMS 932, 72 pp.
- Sheffield, J., E. F. Wood, and M. L. Roderick, 2012: Little change in global drought over the past 60 years. *Nature*, 491, 435– 438, https://doi.org/10.1038/nature11575.
- Stocks, B. J., T. J. Lynham, B. D. Lawson, M. E. Alexander, C. E. V. Wagner, R. S. McAlpine, and D. E. Dubé, 1989: The Canadian forest fire danger rating system: An overview. For. Chron., 65, 450–457, https://doi.org/10.5558/tfc65450-6.
- Tang, Y., S. Zhong, L. Luo, X. Bian, W. E. Heilman, and J. Winkler, 2015: The potential impact of regional climate change on fire weather in the United States. *Ann. Assoc. Amer. Geogr.*, **105** (1), 1–21, https://doi.org/10.1080/00045608.2014.968892.
- Taylor, S. W., and M. E. Alexander, 2006: Science, technology, and human factors in fire danger rating: The Canadian experience. *Int. J. Wildland Fire*, 15, 121–135, https://doi.org/10.1071/WF05021.
- Terando, A., D. Reidmiller, S. W. Hostetler, J. S. Littell, T. D. Beard Jr., S. R. Weiskopf, J. Belnap, and G. S. Plumlee, 2020: Using information from global climate models to inform policymaking—The role of the U.S. Geological Survey. U.S. Geological Survey Open-File Rep. 2020–1058, 32 pp., https://doi.org/10.3133/ofr20201058.
- Van Vliet, L., J. Fyke, S. Nakoneczny, T. Q. Murdock, and P. Jafarpur, 2024: Developing user-informed fire weather projections for Canada. *Climate Serv.*, 35, 100505, https://doi.org/10.1016/j.cliser.2024.100505.
- Van Wagner, C. E., 1987: Development and structure of the Canadian forest fire weather index system. Canadian Forestry Service Forestry Tech. Rep. 35, 37 pp.
- Westerling, A. L., 2016: Increasing western US forest wildfire activity: Sensitivity to changes in the timing of spring. *Philos. Trans. Roy. Soc.*, **B371**, 20150178, https://doi.org/10.1098/rstb. 2015.0178.
- Williams, A. P., J. T. Abatzoglou, A. Gershunov, J. Guzman-Morales, D. A. Bishop, J. K. Balch, and D. P. Lettenmaier, 2019: Observed impacts of anthropogenic climate change on wildfire in California. *Earth's Future*, 7, 892–910, https://doi. org/10.1029/2019EF001210.
- Wotton, B. M., and M. D. Flannigan, 1993: Length of the fire season in a changing climate. For. Chron., 69, 187–192, https://doi.org/10.5558/tfc69187-2.
- Yu, G., Y. Feng, J. Wang, and D. B. Wright, 2023: Performance of fire danger indices and their utility in predicting future wildfire danger over the conterminous United States. *Earth's Future*, 11, e2023EF003823, https://doi.org/10.1029/2023EF003823.